Contrib Mineral Petrol (1998) 130: 162–175

S. Poli · M.W. Schmidt

The high-pressure stability of zoisite and phase relationships of zoisite-bearing assemblages

Received: 23 December 1996 / Accepted: 29 August 1997

Abstract The fluid-absent reaction 12 zoisite = 3 lawsonite + 7 grossular + 8 kyanite + 1 coesite was experimentally reversed in the model system CaO-Al_2O_3-SiO_2-H_2O (CASH) using a multi-anvil apparatus. The upper pressure stability limit for zoisite was found to extend to 5.0 GPa at 700 °C and to 6.6 GPa at 950 °C. Additional experiments both in the H_2O-SiO_2-saturated and in the H_2O-Al_2O_3-saturated portions of CASH provide further constraints on high pressure phase relationships of lawsonite, zoisite, grossular, kyanite, coesite, and an aqueous fluid. Consistency of the present experiments with the H_2O-saturated breakdown of lawsonite is demonstrated by thermodynamic analysis using linear programming techniques. Two sets of data consistent with databases of Berman (1988) and Holland and Powell (1990) were retrieved combining experimental phase relationships, calorimetric constraints, and recently measured elastic properties of solid phases. The best fits result in $G_{f,1,298}^{\circ,\text{zoisite}} = -6,499,400$ J and $S_{1,298}^{\circ,\text{zoisite}} = 302$ J/K, and $G_{f,1,298}^{\circ,\text{lawsonite}} = -4,514,600$ J and $S_{1,298}^{\circ,\text{lawsonite}} = 220$ J/K for the dataset of Holland and Powell, and $G_{f,1,298}^{\circ,\text{zoisite}} = -6,492,120$ J and $S_{1,298}^{\circ,\text{zoisite}} = 304$ J/K, and $G_{f,1,298}^{\circ,\text{lawsonite}} = -4,513,000$ J and $S_{1,298}^{\circ,\text{lawsonite}} = 218$ J/K for the dataset of Berman. Examples of the usage of zoisite as a geohygrometer and as a geobarometer in rocks metamorphosed at eclogite facies conditions are worked, profiting from the thermodynamic properties retrieved here.

S. Poli (✉)
Dipartimento Scienze della Terra, Università di Milano,
Via Botticelli 23, I-20133 Milano, Italy, Tel: ++39 2 23698324;
Fax: ++39 2 70638681; e-mail: stefano@biko.terra.unimi.it

M.W. Schmidt
CNRS-UMR6524, Magmas et Volcans, 5 rue Kessler,
F-63038 Clermont-Ferrand, France, Tel: ++33 4 73.34.67.26;
Fax ++33 4 73.34.67.44; e-mail: max@opgc.univ-bpclermont.fr

Editorial responsibility: V. Trommsdorff

Introduction

Zoisite and clinozoisite, the polymorphs of $Ca_2Al_3Si_3O_{12}(OH)$, are common rock forming minerals. Even though as minor constituents, they are ubiquitous in mafic, intermediate and acidic rocks as well as in calcsilicates when metamorphosed at greenschist, amphibolite and eclogite facies conditions (see review by Deer et al. 1986). In natural rocks where Fe is present, orthorhombic zoisite is typical for eclogite facies whereas clinozoisite or epidote occurs at low to intermediate pressure conditions. In the synthetic CaO-Al_2O_3-SiO_2-H_2O system (CASH), attempts to determine the location of the transformation from orthorhombic zoisite to clinozoisite were strongly affected by low reaction kinetics (Chatterjee et al. 1984; Jenkins et al. 1985). The stability of clinozoisite in Fe-free systems is still questionable as most experiments in CASH result in zoisite growth (Pistorius et al. 1962; Newton 1966; Chatterjee et al. 1984; Jenkins et al. 1985). In CASH, clinozoisite is most likely stable below 350 °C (Jenkins et al. 1985), a temperature which hinders reversal experiments.

At pressures below ca. 0.9 GPa zoisite decomposes to anorthite + grossular + corundum + water through a reaction with positive dP/dT slope (Chatterjee et al. 1984); at higher pressures zoisite destabilizes with temperature through a fluid-absent melting reaction above 1000 °C (Boettcher 1970). Schreinemakers' analysis on the basis of the lawsonite stability (Schmidt and Poli 1994) together with results from H_2O-saturated experiments suggests a maximum pressure stability of zoisite of ca. 7 GPa at 1000 °C.

As a result of its large stability field and its common occurrence, zoisite has been largely used to depict the metamorphic history of both continental and oceanic crust during many geodynamic processes. Zoisite is a buffer phase for various net-transfer reactions involving Ca-bearing solid solution phases used in geothermobarometry, e.g. anorthite component in plagioclase in

assemblage with kyanite and quartz (Goldsmith 1982), or grossular component in garnet at pressures exceeding plagioclase stability (Chopin et al. 1991; Okay 1995). In H_2O-undersaturated assemblages it is also used as a geohygrometer when fluid compositions are obtained from phase equilibria constraints (Rice and Ferry 1982).

Zoisite has also been considered to be an important water reservoir in subducted oceanic crust by Nicholls and Ringwood (1973). They proposed that zoisite is stable to higher pressures than amphibole and thus in subducted crust zoisite may transport and release water to the mantle wedge to greater depth than amphibole. This proposition was confirmed by experiments of Poli and Schmidt (1995) on model basaltic systems. Furthermore, geothermal gradients related to subduction of young and hot oceanic crust may lead to fluid-absent melting of both zoisite and amphibole, generating peraluminous melts (Thompson and Ellis 1994).

Despite such a widespread involvement in the medium- to high-pressure evolution of crustal rocks, the zoisite stability field is still incompletely determined, its upper pressure occurrence is only constrained on the basis of Schreinemakers' analysis (Schmidt and Poli 1994) and computations using available thermodynamic data.

At temperatures lower than ca. 1000 °C, within the stability field of lawsonite, zoisite breaks down with pressure according to a water-absent reaction

$$12\,\text{zoisite} = 3\,\text{lawsonite} + 7\,\text{grossular} + 8\,\text{kyanite} + 1\,\text{coesite}. \quad (1)$$

Calculations using available thermodynamic databases (Berman 1988, updated 1992; Holland and Powell 1990, updated 1994; Holland et al. 1996) locate this reaction at ca. 4.2 GPa at 860 °C (see Fig. 7 in Holland et al. 1996), i.e. about 2.5 GPa lower than inferred by Schmidt and Poli (1994).

The purpose of this study is to determine experimentally *P-T* conditions of the breakdown of zoisite with pressure and to calculate thermodynamic properties of zoisite and lawsonite at high pressures employing recently determined bulk moduli and thermal expansions of zoisite, lawsonite and kyanite. Phase relationships of both H_2O-saturated and H_2O-undersaturated zoisite-bearing assemblages are delineated in order to make our results applicable to a wide spectrum of metamorphic conditions.

Experimental techniques

Most experiments were performed with mixtures of crystalline phases. In reversal experiments all phases participating in the reaction were already present in the starting material. Synthetic lawsonite, zoisite, grossular, and coesite or corundum were mixed with natural kyanite and $Al(OH)_3$. The natural kyanite had trace element concentrations below the detection limit of microprobe analysis. The $Al(OH)_3$ was employed as a source of H_2O. It allows for the addition of precise amounts of H_2O since $Al(OH)_3$ does not dehydrate during welding of the small capsules. $Al(OH)_3$ immediately decomposes during heating and reacts with the other phases present. Zoisite decomposes below 1000 °C through the water-absent reaction (1), thus, bulk compositions for investigation of this reaction were located in the fluid-absent region, i.e. in the quadrangles lawsonite-zoisite-grossular-coesite, lawsonite-zoisite-kyanite-coesite, and zoisite-kyanite-grossular-coesite (Fig. 1). Experiments were also performed on pure zoisite, as will be shown below, they clearly yielded a large metastability of zoisite. A direct test if capsules did leak during the experiment was not possible since a free fluid phase was not present in the experiments.

Capsules were made either of Pt or Au tubing, diameters were 1.6 or 2.0 mm OD. All capsules were welded after loading the fine powdered (< 10 micrometre) starting materials. Capsules were 1 to 1.5 mm long before the experiments and contained 3–5 mg material. Experiments were performed using a split sphere and a split-cylinder multi anvil (MA-8), WC-cubes had edge lengths of 32 mm and truncation edge lengths (TEL) of 17 mm. Assemblies were composed by pyrophyllite gaskets, a prefabricated MgO-octahedron (containing 5 wt% Cr_2O_3) with 25 mm edge length, and a zirconia sleeving containing a stepped graphite heater (Fig. 2). A MgO sleeve was placed between capsules and graphite. The space available for capsules in the central thickened graphite part was 3 mm in height and 3 mm in diameter. Either two 2.0 mm OD or three 1.6 mm OD capsules could be loaded simultaneously.

The length of the capsules was only about half the length of the thickened part of the furnace in order to further diminish thermal gradients (see Fig. 2). An MgO-disk was placed at the bottom and a MgO-ring at the top of the capsules. The axial thermocouple (Pt-Pt90Rh10, S-type) was placed in direct contact with the capsules, a mullite thermocouple-ceramic was used. Thermal gradients over the length of the capsule in this relatively large assembly are less than 20–30 °C at experimental temperatures of 700–1050 °C. An experiment with two axial thermocouples, one thermocouple junction placed in the geometrical centre of the furnace, the second 1 mm apart, yielded differences of 10 (at 300 °C) to 30 °C (at

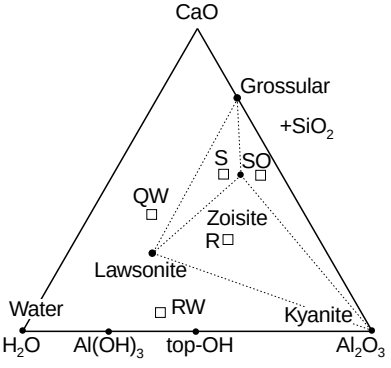

Fig. 1 Starting material mixtures in the system CaO-Al_2O_3-H_2O projected through SiO_2. See caption to Table 1 for details on *S*, *SO*, *QW*, *R*, *RW* starting material compositions

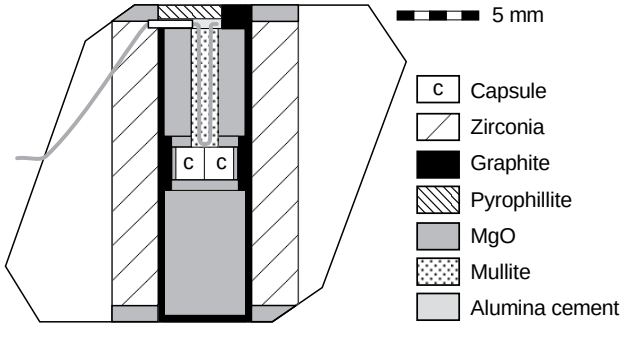

Fig. 2 Cell assembly for multi-anvil experiments, octahedron with an edge length of 25 mm, truncation edge length 17 mm

1100 °C). No corrections were applied to the effects of the pressure on the e.m.f. of the thermocouple. The possibility of loading two or three capsules with different bulk compositions in each experiment was used to test different mixtures of starting materials. However, in few runs at 850 °C and at 900 °C, a mixture of garnet and perovskite structured $CaGeO_3$ was loaded in one of the three capsules. The result (Table 1) was pure perovskite structured $CaGeO_3$ in runs sc08 and sc19 (in the other two capsules of the same experiments lawsonite + grossular + coesite + kyanite were stable instead of zoisite) and pure garnet structured $CaGeO_3$ in run sc10 (in the other two capsules of the experiment zoisite was stable). Thus, between 850 and 900 °C, reaction (1) intersects with the garnet-perovskite structure transition in $CaGeO_3$.

Pressure was calibrated against coesite-stishovite (Zhang et al. 1996), $CaGeO_3$-garnet-perovskite (Susaki et al. 1985), α-β Fe_2SiO_4 (Katsura and Ito 1989; Yagi et al. 1987), and coesite-quartz (Bohlen and Boettcher 1982). Cumulative uncertainties depend largely on the accuracy of the reactions used as calibrant, generally a value of ±4% is assumed.

Run products were analysed using standard powder diffraction techniques.

Results

The terminal pressure stability of zoisite was determined at 700, 850 and 950 °C in a SiO_2-saturated and H_2O-undersaturated CASH system. Experiments are listed in

Table 1 Run table (*zo* zoisite, *law* lawsonite, *ky* kyanite, *gr* grossular, *coe* coesite, *sti* stishovite, *cor* corundum); (-) indicates minor amounts of the phase, and (–) traces at the limit of detection for conventional powder XRD (~ 2%). Starting materials (*st. mat.*) are: *X* and *Y* – zo, $Al(OH)_3$, ky, gr; *RW* and *QW* – gr, ky, qz, $Al(OH)_3$, law, zo, H_2O; *R* – gr, ky, qz, $Al(OH)_3$, law, zo; *S* and *SO* – gr, $Al(OH)_3$, ky, qz, law, zo, dry glass of zoisite composition. Relative proportions of the phases for silica-saturated starting materials can be evaluated from Fig. 1

Run	*P* (GPa)	*T* (°C)	*t* (h)	St. mat.	Results
H_2O- and Al_2O_3-saturated					
Iwma75	6.6	1025	7	X	Zo, ky, cor
Iwma76	6.9	1040	9	X	Zo, ky, cor
Iwma77	6.9	1040	9	Y	Zo, ky, cor
Iwma78	7.2	1060	8	X	Gr, ky, cor
Iwma79	7.2	1060	8	Y	Gr, ky, cor
H_2O- and SiO_2-saturated					
Iwma46	6.1	900	6	RW	Law, ky, coe
Iwma43	6.2	950	2	QW	Law, gr, coe(-)
Iwma42	6.9	950	3	QW	Law, gr, coe(-)
H_2O-undersaturated and SiO_2-saturated					
Iwma47	9.4	1000	3	R	Law, ky, gr(-), sti(-)
Iwma41	6.9	950	3	R	Law, ky, gr(-), coe(-)
Iwma44	6.2	950	2	S	Zo, gr, ky, coes, law(-)
Iwma48	8.6	900	3	S	Law, gr, ky, sti
Iwma45	6.1	900	6	SO	Zo, gr, ky(-), coe(-)
Iwma73	6.5	850	11	SO	Law, zo, gr, ky, coe
Iwma74	6.5	850	11	R	Law, zo, gr, ky, coe
Iwma68	6.3	850	14	R	Law, zo, gr, ky, coe
Iwma63	6.0	850	10	R	Zo, law, gr, ky, coe
Iwma64	6.0	850	10	SO	Zo, gr, ky, coe
Iwma80	6.0	800	58	R	Law, gr, ky, coe
Iwma81	6.0	800	58	S	Law, gr, ky, coe
Iwma60	7.4	700	4	SO	Law, ky, gr, coe, zo(-)
Iwma58	6.9	700	5	SO	Law, zo, gr, ky, coe
Iwma56	6.6	700	3	SO	Law, gr, ky, coe, zo(–)
Iwma54	6.2	700	4	SO	Law, zo, gr, ky, coe
Iwma51	5.95	700	3	R	Law, gr, ky, coe
Iwma50	5.7	700	3	R	Law, gr, ky, coe
Iwma71	5.35	700	8	R	Law, zo, gr, coe, ky(-)
Iwma72	5.35	700	8	SO	Law, gr, ky, coe
Iwma66	5.0	700	12	R	Zo, law, gr, coe, ky(-)
Iwma67	5.0	700	12	SO	Zo, gr, ky, coe
Experiments on pure synthetic zoisite					
Iwma65	6.0	850	10	Zoisite	Zo
Iwma69	6.3	850	14	Zoisite	Zo
Iwma49	5.7	700	3	Zoisite	Zo
Iwma52	5.95	700	3	Zoisite	Zo
Iwma53	6.25	700	4	Zoisite	Zo
Iwma55	6.6	700	3	Zoisite	Zo
Iwma57	6.9	700	5	Zoisite	Zo
Iwma59	7.4	700	4	Zoisite	Zo, law(-), gr(-),ky(-), coe(-)
Calibration experiments					
sc08	6.2	950	2	$CaGeO_3$	Perovskite structure
sc09	6.9	950	3	$CaGeO_3$	Perovskite structure
sc10	6.1	900	6	$CaGeO_3$	Garnet structure
sc15	6.2	700	4	$CaGeO_3$	Garnet structure
sc19	6.5	850	11	$CaGeO_3$	Perovskite structure

Table 1 and results presented in Fig. 3. Zoisite was found to be stable to ca. 5 GPa at 700 °C and to ca. 6.6 GPa at 950 °C, at higher pressures it decomposed to lawsonite + grossular + kyanite + coesite (reaction 1).

The experiments on the fluid-absent reaction (1) proved to be more difficult than expected. Reaction rates were slow and complete reaction was not always obtained. Run products with relatively small reaction rates were examined by SEM. However, unequivocal reaction textures or replacement structures could not be observed. For most reversal experiments (Table 1) direction of reaction could clearly be identified by comparing relative X-ray diffraction peak heights of starting materials and experimental products.

For each pressure-temperature condition two or three different starting materials were loaded. One of the starting materials was synthetic zoisite. This starting material never reacted fully (see Table 1), zoisite proved to be extremely metastable and persisted even 2 GPa above its reversed equilibrium stability.

In order to have an independent test on the pressure effect on zoisite stability, we also determined a zoisite breakdown reaction in an Al_2O_3 + H_2O-saturated system. The reaction

$$6 \text{ zoisite} + 1 \text{ corundum} = 4 \text{ grossular} + 6 \text{ kyanite} + 3 \text{ } H_2O \quad (2)$$

was determined to locate between 6.9 GPa and 7.2 GPa at 1040 °C. Because reaction (2) has to lie at pressures lower than its SiO_2-saturated equivalent

$$6 \text{ zoisite} = 4 \text{ grossular} + 5 \text{ kyanite} + 1 \text{ coesite} + 3 \text{ } H_2O \quad (3)$$

the experimental bracket on reaction (2) at 1040 °C (stars in Fig. 3) also constrains the lowermost location of reaction (3).

Because reactions (2) and (3) are stable over a narrow temperature range of ca. 50 °C, it is not possible experimentally to determine their dP/dT slope. At temperatures higher than 1050 °C, eutectic melting of zoisite + coesite + kyanite + H_2O (Boettcher 1970; Schmidt and Poli 1994) occurs. Our experimental results on reactions (1) and (2) are consistent with our previous experiments on the stability of lawsonite (Schmidt and Poli 1994; Schmidt 1995). They are, within the temperature uncertainty, also consistent with the determination of the breakdown reaction of lawsonite to zoisite + kyanite + coesite + water by Skrok et al. (1994) (see Fig. 3).

The dP/dT slope of the breakdown reaction of lawsonite to grossular + kyanite + coesite + water is still not well constrained. One single experiment by Pawley (1994) at 9 GPa, 1050 °C yielded lawsonite unstable but the estimated error on temperature in this experiment is in the order of 100 °C and lawsonite was present as a run product at the cold ends of the capsule.

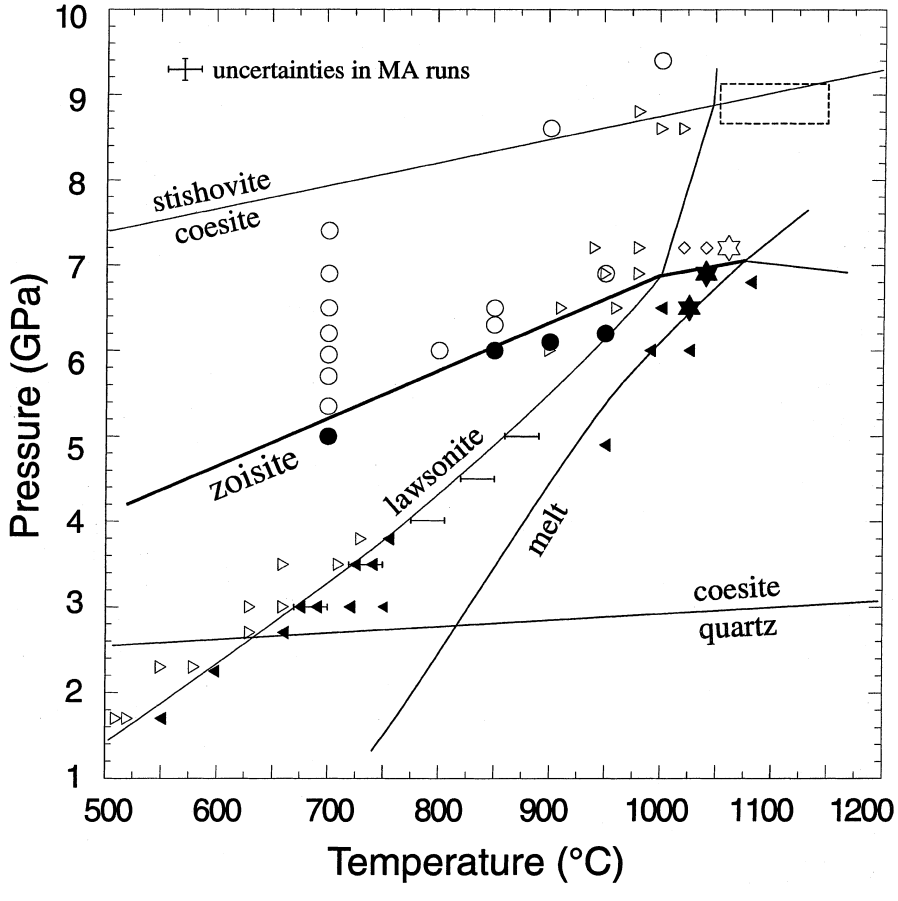

Fig. 3 Experimentally determined phase relationships from 1 to 10 GPa in the model system CASH. (*Circles* H_2O-undersaturated and SiO_2-saturated *open circles* lawsonite + grossular + kyanite + coesite, *full circles* zoisite. *Triangles and diamonds* H_2O- and SiO_2-saturated: *open triangles* lawsonite, *full triangles* zoisite + kyanite + coesite/quartz, diamonds grossular + kyanite + coesite + H_2O. *Stars* H_2O- and Al_2O_3-saturated: *full stars* zoisite + corundum + kyanite + H_2O, *open star* grossular + coesite + kyanite + H_2O. *Horizontal bars* experiments from Skrok et al., 1994, *small symbols* selected runs from Schmidt and Poli, 1994, *dashed box at 9 GPa* assemblage grossular + kyanite + coesite/stishovite obtained by Pawley, 1994)

Thermodynamic analysis

We calculate two sets of thermodynamic properties for zoisite and lawsonite consistent with the database of Holland and Powell (1990, updated 1994) and of Berman (1988, updated 1992), respectively. Consequently, we use two sets of entropies, C_P functions, and Gibbs free energies for kyanite, grossular, anorthite, and coesite. Entropy and free energy of stishovite is from Schmidt et al. (1997) following Akaogi et al. (1995). Elastic properties are listed in Table 2. In the following we discuss the thermodynamic properties of lawsonite and zoisite in detail.

Entropies and C_P-functions

Standard state entropies ($S^{\circ,\text{zoisite}}_{1,298}$ and $S^{\circ,\text{lawsonite}}_{1,298}$) and C_P-functions of zoisite and lawsonite were measured by Perkins et al. (1980). For zoisite Perkins et al. obtained a smooth C_P function. On the contrary, the calorimetric measurement of lawsonite did encounter several problems at temperatures below 298.15 K. The lawsonite sample used by Perkins et al. (1980) contained fluid inclusions and the discontinuities observed in the C_P function at 120–130 K and 270–275 K were assigned to an ice phase transition and to the melting of ice. A correction for 0.5 wt% H_2O was applied by Perkins et al. (1980) to the experimental measurements. The recent discovery of low-temperature phase transitions in lawsonite at 155 K and 273 K (Libowitzky and Armbruster 1995) renders additional corrections necessary and may suggest a re-interpretation of the discontinuities in heat capacity measurements of Perkins et al. (1980). However, since both phase transitions in lawsonite are displacive and probably second order lambda transitions (Thompson and Perkins 1981), detailed calorimetry is necessary in the vicinity of the phase transitions.

Additional problems with the entropy of lawsonite are: a non-zero entropy at 0 K can be observed on a C_P/T versus T plot after fitting data below 15 K. It is unclear, if this behaviour is caused by ordering of hydrogen in lawsonite or by the presence of ice (which exhibits a typical "residue" entropy close to 0 K). Secondly, the phase transition observed at 155 K by Libowitzky and Armbruster (1995) does not match the C_P-discontinuity at 120–130 K of Perkins et al. (1980). Furthermore, the 273 K transition in lawsonite superimposes the water-ice transition. Any of these phase transitions in lawsonite would increase the standard state entropy of lawsonite. However, the smoothing of the C_P function and the correction for ice/water as calculated by Perkins et al. (1980) might lead to an overestimation of the standard state entropy of lawsonite. Thus, the overall effect of the various necessary corrections on the lawsonite standard state entropy remains unresolved. In conclusion, we thus consider the error of standard state entropy for lawsonite relatively large.

The C_P function of lawsonite and zoisite at high temperatures

Even though heat capacities for all of the phases involved in this study were measured, the extrapolation of calorimetric data on hydrous phases to high temperatures strongly depends on the polynom used for the C_P function and if physical constraints are applied to the high-temperature portion of the C_P-function. This is

Table 2 Elastic and thermal properties for solid phases and C_P-functions of lawsonite and zoisite used as fixed input parameters for retrieval calculations

	$V^{\circ}_{1,298}$ (J MPa^{-1})	$K_{T(298)}$ (GPa)	K′	$\alpha = \alpha_0 + \alpha_1 T + \alpha_2 T^{-1} + \alpha_3 T^{-2}$			
				$\alpha_0 \times 10^5$	$\alpha_1 \times 10^8$	$\alpha_2 \times 10^2$	$\alpha_3 \times 10^1$
Zoisite	13.61[a]	102.0[a]	4.8[a]	3.860[b]	–	–	–
Lawsonite	10.15[b]	96.0[c]	4.0[c]	3.130[b,c]	–	–	–
Kyanite	44.14[d]	156.0[d]	5.6[d]	2.443[e]	–	3.936	–
Stishovite	14.01[f]	315.0[g]	5.3[g]	1.053[h]	0.903	–	1.220
Coesite	20.64[f]	96.0[i]	8.4[i]	0.543[h]	0.500	–	–
Grossular	125.35[f]	168.0[j]	6.2[j]	1.951[k]	0.809	–	−0.497

	$C_P = a + bT^{-0.5} + cT^{-2} + dT^{-3}$			
	a	b	c × 10^{-7}	d × 10^{-9}
Zoisite	718.11[l]	−5184.8	−1.3593	2.3077
Lawsonite	539.23[l]	−1523.7	−3.9553	7.2389

[a] Comodi and Zanazzi (1997)
[b] Pawley et al. (1996)
[c] Comodi and Zanazzi (1996)
[d] Comodi et al. (1997)
[e] Fitted to data of Winter and Ghose (1979)
[f] Robie et al. (1978)
[g] Li et al. (1997)
[h] Akaogi et al. (1995)
[i] Levien and Prewitt (1981)
[j] Knittle (1995)
[k] Fei (1995)
[l] This study

particularly relevant for lawsonite since the metastable persistence of lawsonite (or zoisite) at atmospheric pressure extends only to 327 °C (for zoisite to 456 °C) and calorimetric measurements at higher temperatures are not feasible. Nevertheless, at high pressure, the lawsonite stability field extends to more than 1000 °C and that of zoisite to more than 1100 °C. In order to perform calculations at temperatures largely beyond the measured range, C_P functions must be extrapolated on a physical basis. It is known that C_V convergences at high temperatures to $3nR$ according to the law of Dulong and Petit, and consequently C_P to $3nR + \alpha^2 V T K_T$. Anharmonic contributions and ordering terms for most silicates account for less than a few percent of C_P above the Debye temperature, electronic or magnetic contributions are expected to be unimportant in lawsonite and zoisite. Therefore the limit of Dulong and Petit represents a useful approximation for these phases.

Recently determined elastic properties for both zoisite and lawsonite (Pawley et al. 1996; Comodi and Zanazzi 1996, 1997) permit to fit the original calorimetric data of Perkins et al. (1980) together with a reliable high-temperature constraint. We prefer a 4-parameter polynom for C_P as given by Berman and Brown (1985) (see Table 2); it fits the measurements and high-temperature convergence criteria. Extended 7-parameter polynoms for C_P (e.g. Saxena et al. 1994) did not yield any improvement in the fit. Figure 4 illustrates C_P functions for lawsonite used in the literature and our C_P function based on the measurements of Perkins et al. (1980) for low temperatures and extrapolated following the high-temperature convergence criteria. A large deviation of the curve of Perkins et al. (1980) is related to the usage of a Mayer-Kelley equation which is known to be unsuitable for extrapolations. The difference between our fit and the one of Berman (1988) is in the order of 7% at 1200 K. Such a difference causes a displacement of the invariant point in Fig. 3 by ca. 50 °C. The C_P function employed by Holland and Powell (1990) decreases above 1300 K which is physically unreasonable. Differences for C_P functions of zoisite from Berman (1989), Holland and Powell (1990) and our fit (which takes into account the high-temperature convergence criterion) are relatively small, probably because high-temperature phase equilibria for zoisite are available.

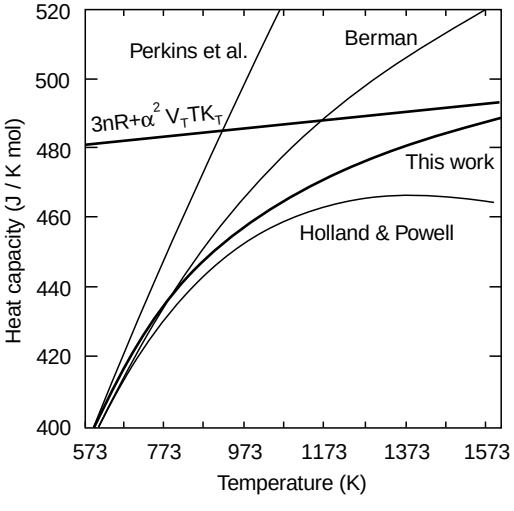

Fig. 4 Comparison of heat capacity (C_P) functions for lawsonite with the law of Dulong and Petit using $n = 19$, $V_T = V_{1,298}(1 + \alpha(T-298))$, R = gas constant, $K_T = 110$ GPa (bulk modulus determined by Comodi and Zanazzi, 1996). *Curve* labelled *Perkins et al.* is from Perkins et al. (1980), *Berman* from Berman (1988 updated 1992) and *Holland & Powell* from Holland and Powell (1990, updated 1994)

Volume equation of state of solids

A Murnaghan equation of state was used to calculate volumes of solid phases at pressure and temperature. Temperature derivatives of bulk modulus at constant pressure $[(dK/dT)_P]$ for all phases involved in this study are unknown. Therefore we assume $(dK/dT)_P = 0$ for all phases. This simplification does have a small effect on calculations at temperatures to 1000 °C. The temperature dependence of bulk modulus is probably in the order of −10 to −40 MPa/K and results in shifts of calculated positions of reactions in the order of 10 °C or some 100 bar with respect to calculations setting $(dK/dT)_P = 0$ for all of the phases. Thus, as long as $(dK/dT)_P$ is not directly measured, setting $(dK/dT)_P = 0$ for all phases yields more consistent results than estimations (currently not available for lawsonite and zoisite).

Thermal expansions (α), bulk moduli (K_T) and pressure derivatives of bulk moduli at constant temperature (K') for zoisite and lawsonite were recently determined by Grevel et al. (1996), Comodi and Zanazzi (1996, 1997), Pawley et al. (1996), and Holland et al. (1996). While thermal expansion coefficients for lawsonite determined by Pawley et al. (1996) and Comodi and Zanazzi (1996) are essentially identical ($3.16 \cdot 10^{-5}$, and $3.13 \cdot 10^{-5}$, respectively), the bulk modulus obtained by Holland et al. (1996, $K_T = 194$ GPa) is much higher than those of Comodi and Zanazzi (1996, $K_T = 96$ GPa, $K' = 4$) and Grevel et al. (1996, $K_T = 91$ GPa).

An important overestimation of bulk moduli in the study of Holland et al. (1996) can be deduced from their data on zoisite-polymorphs. Holland et al. (1996) found a K_T for zoisite of 279 GPa (a value higher than the one for corundum), which is 80% higher than their bulk modulus for clinozoisite (154 GPa). The transformation between the two polytypes is related to the stacking sequence and a slight modification in the octahedral chains, thus a very similar compression behaviour can be expected. Zoisite and clinozoisite have the same chemical formula. Therefore, C_P functions should be very similar (maximum deviations in the order of 5%; see Helgeson et al. 1978, and Berman and Brown 1985), they are actually assumed to be identical in most thermody-

namic databases. Because thermal behaviour of orthorhombic zoisite and clinozoisite is roughly similar, the 80% difference in K_T should result in completely different heat capacities at high temperatures (limit of Dulong and Petit), a fact which is in strong contradiction with the previous evidence. Furthermore, Anderson (1989) demonstrated that bulk moduli of silicates can be determined through an approximation on the basis of density and mean atomic weight, both being very similar in ortho- and clinozoisite. As a consequence, for lawsonite and zoisite we employ compressibilities obtained by DAC single crystal refinement by Comodi and Zanazzi (1996, 1997) ($K_T^{\text{zoisite}} = 102$ GPa). Compressibilities and expansivities for grossular, kyanite, stishovite, coesite are listed in Table 2. The use of a Murnaghan equation of state does not alter the consistency of other thermodynamic properties for such phases with the databases of Holland and Powell, and of Berman. A Murnaghan equation of state allows to reproduce their elastic properties at low pressure but to improve prediction at pressures higher than 1 GPa. Differences of computed volumes from Eq. 5 in Berman (1988) or the formulation in Holland and Powell (1990, page 91), and a Murnaghan equation of state at $P < 1$ GPa and $T < 1573$ K are always less than 0.2%.

Equation of state for fluids

Zoisite breakdown with pressure through reaction (1) does not involve a free H_2O phase. However, the calculation of phase relationships in the CASH model system and refinement of thermodynamic properties of zoisite and lawsonite requires a suitable equation of state (EoS) for water at high pressure. Several equations of state for water at pressures higher than 4 GPa are currently available, even though substantially untested (Delany and Helgeson 1978; Halbach and Chatterjee 1982; Saxena and Fei 1987a,b; Brodholt and Wood 1993; Frost and Wood (in press); Holland and Powell 1991, adjusted with new virial term coefficients in Holland et al. 1996). Any of these equations of state permit the retrieval of thermodynamic properties for zoisite and lawsonite consistent with experimental data. However, because equations of Delany and Helgeson (1978) and Holland and Powell (1991) were used to retrieve the datasets of Berman (1988) and Holland and Powell (1990, updated 1994) respectively, we will forward two sets of data for lawsonite and zoisite consistent with these EoS for water.

A set of thermodynamic data for zoisite and lawsonite

The experimental data of this study were treated along with results from Schmidt and Poli (1994) on the reaction:

$$4\ \text{lawsonite} = 2\ \text{zoisite} + 1\ \text{kyanite} + 1\ \text{quartz/coesite} + 7\ H_2O \quad (4)$$

and with data of Chatterjee et al. (1984) on the reaction:

$$2\ \text{zoisite} + 1\ \text{kyanite} + 1\ \text{quartz} = 4\ \text{anorthite} + 1\ \text{H2O} \quad (5)$$

in order to account for experimental brackets at low pressure.

A linear programming technique was used to verify internal consistency of experimental data and to obtain a feasible region (Gordon 1973) for G° and S° of zoisite and lawsonite as a function of P, T and of the other thermodynamic data previously discussed. Inequalities were placed considering experimental uncertainties. However, a relevant but quantitatively unpredictable reduction of the activity of H_2O with increasing temperature and pressure is expected due to a significant amount of dissolved matter in the fluid (for SiO_2 in quartz/coesite experiments see Manning, 1994). Therefore, during the fit procedure only piston cylinder experiments (Schmidt and Poli 1994) at relatively low temperatures and pressures were employed as constraints on reaction (4).

Because the dP/dT slopes of equilibria (1) and (4) are tightly constrained by our experiments, and volumes are calculated by the well known equations of state for these minerals, fitted $S_{1,298}^{\circ,\text{lawsonite}}$ and $S_{1,298}^{\circ,\text{zoisite}}$ are mathematically correlated. The entropy of zoisite ($S_{1,298}^{\circ,\text{zoisite}} = 297$ J/K) obtained by Perkins et al. (1980) always locates inside the feasible region defined by our experiments, whereas consistent values of $S_{1,298}^{\circ,\text{lawsonite}}$ are always lower than the value obtained by Perkins et al. ($S_{1,298}^{\circ,\text{lawsonite}} = 230$ J/K). As discussed above, a reliable measurement of the standard state entropy of zoisite has been obtained by Perkins et al. (1980), whereas the determination of $S_{1,298}^{\circ,\text{lawsonite}}$ resulted in a large error. Therefore, as an optimization strategy, we adopt an entropy for zoisite within the error of the measurement by Perkins et al. (1980) and we calculate a standard state entropy of lawsonite as close as possible to the problematic value determined by Perkins et al. (1980). Table 3 shows the calculated thermodynamic properties according to the database selected. Application of the EoS for water by Halbach and Chatterjee (1982) results in a higher entropy of lawsonite, whereas a fit using the EoS by Brodholt and Wood (1993) and Frost and Wood (1997)

Table 3 Gibbs free energies of formation from the oxides, and third law entropies for zoisite and lawsonite, consistent with the thermodynamic database of Berman (1988, updated 1992) and Holland and Powell (1990, updated 1994). Units are Joule, K, bar

Database and water EoS	$G_{f,1,298}^{\circ,zoisite}$	$S_{1,298}^{\circ,zoisite}$	$G_{1,298}^{\circ,lawsonite}$	$S_{f,1,298}^{\circ,lawsonite}$
Holland and Powell 1990, 1991; Holland et al. 1996	−6,499,400	302	−4,514,600	220
Berman 1988; Delany and Helgeson 1978	−6,492,120	304	−4,513,000	218

leads to a lower entropy of lawsonite. To what extent such deviations are the consequence of incorrect predictions of water EoS, of unreliable calorimetric measurements on lawsonite, or to decreasing H_2O activity due to the increasing amount of dissolved matter with experimental temperature remains unresolved. Differences among calculated free energies of formation from the elements for both zoisite and lawsonite, and those tabulated in the databases of both Berman (1988) and Holland and Powell (1990, updated 1994) are in the order of 2 kJ and thus within their uncertainties.

Phase relationships in CASH at high pressure

Phase relationships at high pressure in CASH were computed using PeRpLeX package (Connolly 1990), modified to include a Murnaghan EoS for solids and the water EoS listed above. Thermodynamic properties listed in Tables 2 and 3 were employed.

Furthermore, the location of the reaction:

$$1\ \text{kyanite} + 1\ H_2O = 1\ \text{topaz-OH} \quad (6)$$

has been experimentally determined by Wunder et al. (1993) and the intersection of equilibrium (6) with

$$3\ \text{lawsonite} = 1\ \text{grossular} + 2\ \text{kyanite} + 1\ \text{coesite/stishovite} + 6\ H_2O \quad (7)$$

permits to locate an invariant point (Fig. 5, upper right corner) where two reactions generate:

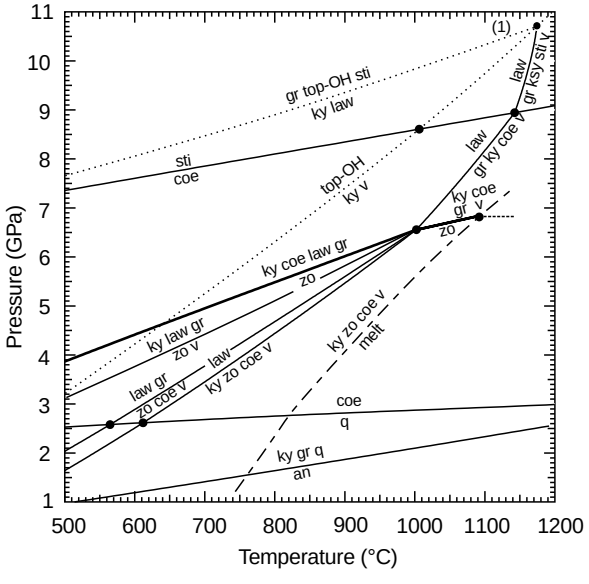

Fig. 5 Computed phase relationships in the SiO_2-saturated portion of the system CASH from 1 to 11 GPa using retrieved thermodynamic properties for lawsonite and zoisite, according to the database of Berman (1988) and the water EoS of Delany and Helgeson (1978). *Heavy lines* indicate reactions which delimit the maximum stability of zoisite. *Dotted lines* are reactions involving topaz-OH as determined after Wunder et al. (1993) and constrained by location of invariant point (1). *Dash-dotted* lines stand for solidus in CASH. (an anorthite, *top-OH* topaz-OH, *v* = water)

$$3\ \text{lawsonite} + 4\ \text{kyanite} = 1\ \text{grossular} + 1\ \text{stishovite} + 6\ \text{topaz-OH} \quad (8)$$

$$3\ \text{lawsonite} = 1\ \text{grossular} + 1\ \text{stishovite} + 2\ \text{topaz-OH} + 4H_2O. \quad (9)$$

The dP/dT slope of equilibria (8) and (9) were obtained after evaluating the standard state entropy of topaz-OH (100 J/K) from the dP/dT slope of reaction (6). All water EoS employed in this study lead to a positive dP/dT slope of equilibrium (7) both with coesite and stishovite. A change of the sign of the dP/dT slope of the lawsonite breakdown reaction appears when kyanite reacts to topaz-OH in the presence of H_2O. The calculated slope of Eq. (8) is strongly affected by the different EoS for water. Experiments at 12 GPa by Schmidt (1995) and Pawley (1994) further constrain the dP/dT slope of reaction (8), but poor knowledge of the thermodynamic properties of topaz-OH hinders calculation of reaction positions in this P-T region. Figure 5 shows that the maximum temperature stability of lawsonite extends to ca. 1100 °C at 10 GPa, in agreement with experimental results of Pawley (1994). Reaction (8) might be the cause of the high-pressure stability limit of lawsonite in intermediate compositions (greywackes) at ca. 9–10 GPa (Poli and Schmidt 1997). This reaction will occur when peraluminous crustal material is subducted in relatively cold subduction zones (Davies and Stevenson 1992). Domanik and Holloway (1997) found lawsonite and topaz-OH to coexist with garnet and clinopyroxene in a metapelite composition at conditions of 6–8 GPa, 700–900 °C. At 8–10 GPa such an assemblage was found to react and lawsonite disappears in agreement with our calculations in the model system CASH.

The computed slope of reaction (3) (Fig. 5) is positive and implies hydration with increasing temperature. Although minor adjustments to entropies and volumes of participating phases are still possible, these adjustments will not change the sign of ΔS and ΔV of reaction because both of them are relatively large (−100 J/K and −2.9 J/bar, respectively).

Zoisite stability and phase relationships in H_2O-undersaturated rocks

The occurrence of zoisite + coesite-bearing assemblages in high-pressure terrains has become manifest, both at H_2O-saturated conditions (Dabie-Shan, China; Okay 1995) and H_2O-undersaturated conditions (Straumen, Norway; Smith 1988, p. 53). In nature, zoisite develops at H_2O-undersaturated condition mostly in coronitic rocks metamorphosed under eclogite or amphibolite facies conditions as a result of uneven H_2O distribution (Rubie 1990). Consequently, zoisite-bearing equilibria have been largely used to decipher fluid composition in orogenic processes s.l. (e.g. Ghent 1988; Powell and Holland 1994). However, zoisite stability in H_2O-un-

dersaturated rocks occurs as the result of two distinct processes: (1) absence of a free fluid phase but presence of hydrous phases (further on referred to as "H_2O-undersaturated – fluid absent"); (2) dilution of H_2O component in a mixed fluid, e.g. H_2O-CO_2 fluid (further on referred to as "H_2O-undersaturated – mixed fluids").

Phase relationships at H_2O-undersaturated – fluid-absent conditions in the model system CASH are entirely described in the phase diagram of Fig. 5. Obviously, some of the reactions in Fig. 5 only occur when H_2O is an excess phase, e.g.

$$5 \text{ lawsonite} + 1 \text{ grossular} = 4 \text{ zoisite} + 1 \text{ coesite} + 8\ H_2O. \quad (10)$$

Other reactions such as our experimentally determined reaction (1) only occur if a fluid phase is absent, the maximum pressure stability of zoisite within the lawsonite stability field can be attained only at H_2O-undersaturated – fluid-absent condition. However, in the CASH system reactions cannot shift in P and T since all solid phases have constant compositions and unit activities.

On the contrary H_2O-undersaturated – mixed-fluid-present conditions cause a displacement of reactions which involve fluid as the activity of H_2O is reduced in a mixed fluid.

The distinction between the two cases above is obvious but has been frequently underevaluated when "fluid compositions" or "H_2O activities" have been indirectly obtained from phase equilibria in rocks. With three independent reactions among the independent components of the phases present in a hydrated rock, three potentials can be obtained: usually P-T, and the chemical potential of H_2O. Common techniques used in the literature to perform such calculations are fixed activity corrections on selected reactions (e.g. Ghent 1988) and multi-equilibrium calculations (e.g. TWEEQU, Berman 1991; THERMOCALC, Powell and Holland 1994). Applications of such techniques usually assume that low "H_2O activities" are related to the presence of a mixed fluid, commonly a H_2O-CO_2 fluid. However, it should be noted that, in contrast to solid phases, the presence or absence of the fluid phase cannot be demonstrated directly (high-pressure fluid inclusions are rarely pre-

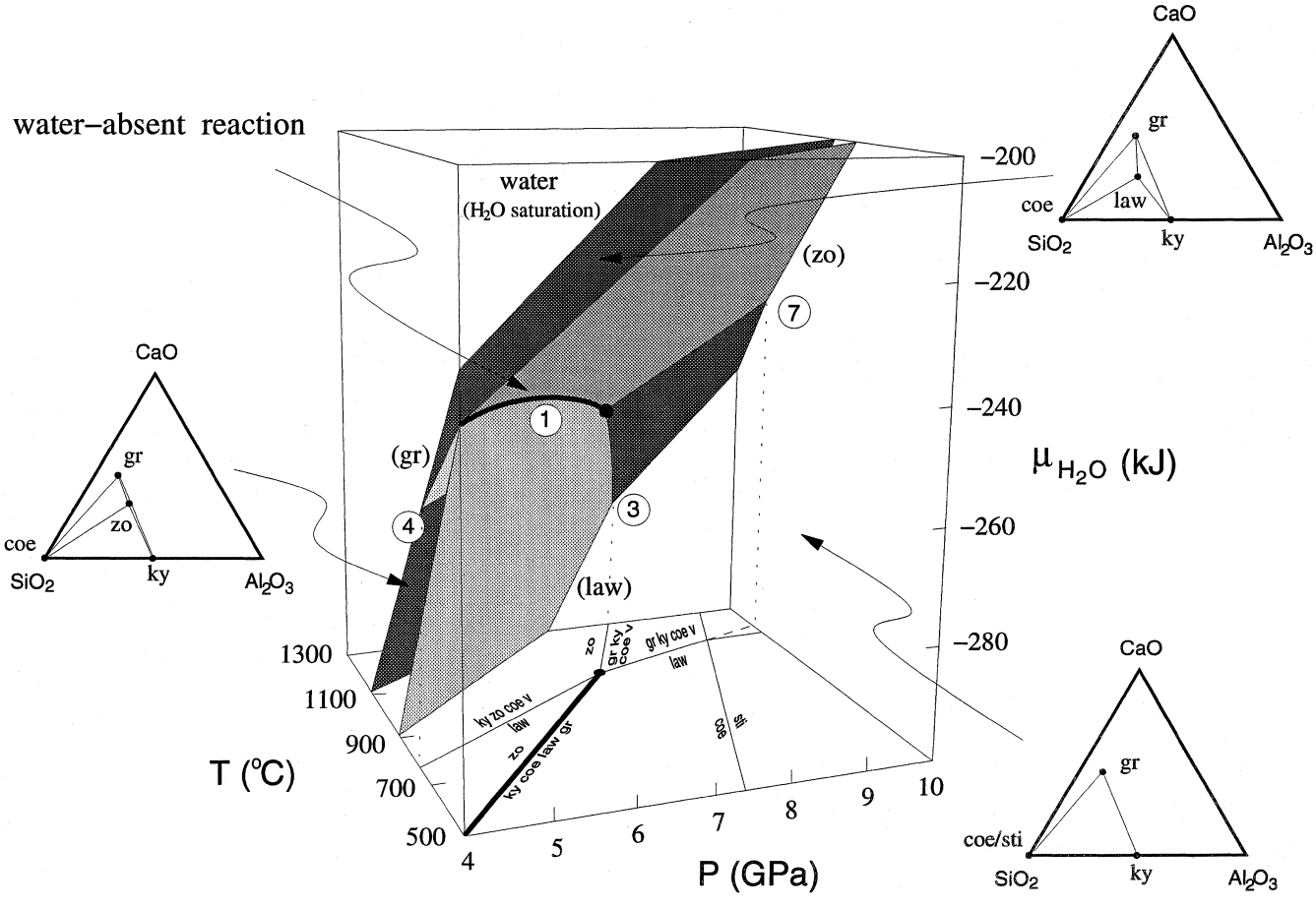

Fig. 6 Property diagram (chemical potential of component H_2O) for the system CASH around the bundle involving lawsonite, zoisite, grossular, kyanite and coesite. The *heavy shaded plane* stands for H_2O properties in a pure aqueous fluid. The *heavy line* represents the locus of $\mu(H_2O)$ buffered by the 5 solid phases involved and corresponds to the "fluid-absent" reaction (1) experimentally determined in this study. Phase relationships projected onto the *base* of the block diagram represent H_2O-saturated conditions. *Numbers in circles* refer to reactions described in the text. CAS composition diagrams illustrate assemblages attending different degrees of H_2O-undersaturation. Abbreviations as in Fig. 5. See text for further explanation

served) and therefore only the chemical potential of H_2O, but not the activity or fraction of H_2O in a fluid, can be calculated. Furthermore, when "multi-equilibrium" calculations are performed, the assemblage chosen is not necessarily stable at the calculated pressure and temperature since the stability of the assemblage is commonly not tested. Whether the $\mu(H_2O)$ calculated has to be referred to H_2O-undersaturated – fluid-absent or to H_2O-undersaturated – mixed-fluid-present conditions should be derived on the basis of phase equilibria constraints.

H_2O-undersaturated – fluid absent

In Figs. 6 and 7 we illustrate the difference between H_2O-undersaturated – fluid-absent and H_2O-undersaturated – mixed – fluid-present conditions in the CASH model system. At each *P-T*, the chemical potential of H_2O is determined either by water ± hydrous phases, or mixed fluid ± hydrous phases, or hydrous phases only. The shaded planes marked (law), (zo), (gr) represent (using Schreinemakers' notation) values of $\mu(H_2O)_{(P,T)}$ when buffered by grossular + kyanite + coesite + zoisite (law), grossular + kyanite + coesite + lawsonite (zo), or kyanite + coesite + zoisite + lawsonite (gr) respectively, e.g.:

$$6\,\mu(H_2O) = 3\,\mu(\text{law}) - 1\,\mu(\text{gr}) - 2\,\mu(\text{ky}) - 1\,\mu(\text{coe})$$
[equilibrium (zo)].

In *P-T*-$\mu(H_2O)$ space the intersection line of this plane with the $\mu(H_2O)_{(P,T)}$ defined by a given EoS for water (the heavy shaded plane in Fig. 6) represents the univariant curve (7) which is projected onto the *P-T* plane.

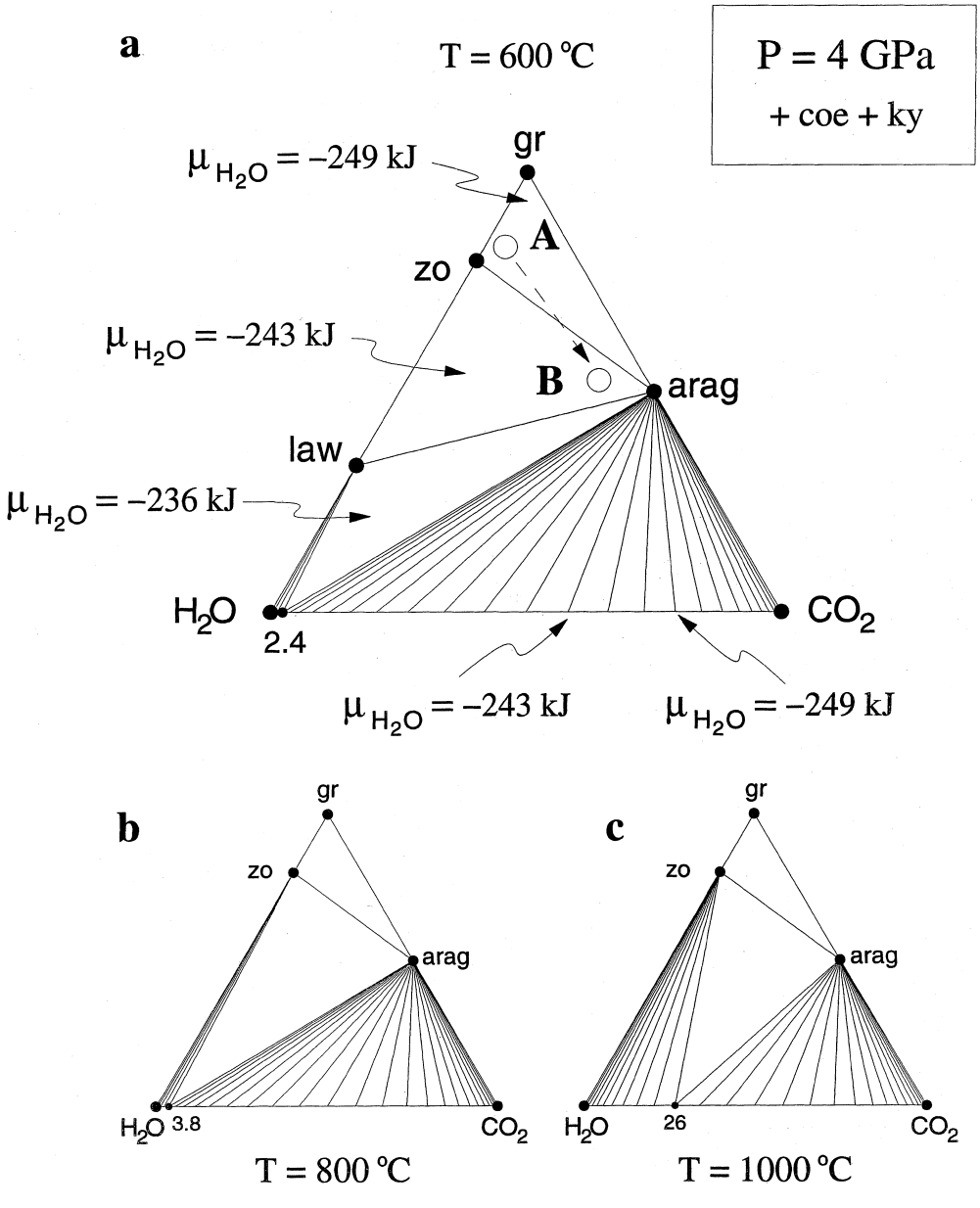

Fig. 7 Composition diagram projected through SiO_2 and Al_2O_3 (i.e. coesite and kyanite on the buffering surface at selected pressure and temperature conditions) which shows occurrence of hydrates and carbonates at fluid-absent conditions, possible equality of $\mu(H_2O)$ in both fluid-absent and fluid-present conditions at different solid phase assemblages, and possible increase of $\mu(H_2O)$ (and formation of the more hydrated phase lawsonite compared to zoisite) by the addition of CO_2 from bulk composition *A* to bulk composition *B*. (*arag* aragonite)

"Saturation" of H_2O is defined by the presence of water, and, if water is in mechanical equilibrium with solids, $P_{water} = P_{solids}$. Above the heavy shaded plane P_{fluid} would be larger than P_{solids} which is only possible in non-equilibrium situations. Consequently, in equilibrium, $\mu(H_2O)$ cannot be increased to values above the heavy shaded plane. On the contrary, a large number of H_2O-undersaturated conditions is possible below the heavy shaded plane, either in the presence or absence of hydrous phases. As an example we consider a pressure of 4 GPa (left face of block diagram in Fig. 6) and a temperature of 600 °C. The assemblage lawsonite + kyanite + coesite may well be in equilibrium at H_2O-undersaturation (upper chemography on the right of Fig. 6, which is valid in the volume bound by the H_2O-saturation plane, the (zo) plane and the (gr) plane). With decreasing $\mu(H_2O)$, zoisite + kyanite + coesite assemblage occurs (chemography on the left), and at very low $\mu(H_2O)$ the anhydrous assemblage grossular + kyanite + coesite becomes stable. The "fluid-absent" reaction (H_2O) is represented by the intersection of the planes (gr), (law), (zo). There, the variance is lowered by the coexistance of 5 phases (zo, ky, coe, law, gr) and the intersection of the univariant curve (1) in P-T- $\mu(H_2O)$ space (Fig. 6) with the water-saturation plane generates the invariant point on the P-T plane of Fig. 6.

If H_2O is the only fluid species, the phase diagram of Fig. 6 is complete for both H_2O-saturated and H_2O-undersaturated – fluid-absent conditions.

H_2O-undersaturated – mixed fluid present

Dilution of H_2O with other components, most commonly CO_2, causes displacement of the "fluid"-saturation plane to lower $\mu(H_2O)$. As a consequence, equilibria (3), (4), and (7), but not equilibrium (1), shift towards lower pressures and lower temperatures, respectively. Addition of CO_2 component to the system enables the appearance of carbonates, e.g. aragonite at high pressure. However, also in an enlarged system with CO_2 as additional component, H_2O-undersaturated conditions and presence of carbonates do not necessitate the existence of a free fluid phase. Figure 7 was calculated in the system CASH + CO_2 and is projected through SiO_2 and Al_2O_3, i.e. coesite and kyanite are present on the saturation surface. Both, H_2O-undersaturated – fluid-absent and H_2O-undersaturated – mixed-fluid-present conditions occur in Fig. 7.

Figure 7a shows that: (1) presence of hydrous phase(s) + carbonate does not imply the presence of a fluid: the assemblages lawsonite-aragonite-zoisite and zoisite-aragonite-grossular do not coexist with a fluid phase. (2) The same chemical potential of component H_2O can be obtained both at H_2O-undersaturated – fluid-absent and H_2O-undersaturated – mixed-fluid conditions. For example, a $\mu(H_2O)$ of −243 kJ is calculated with a dataset consistent with Berman (1988) for the compositional triangle lawsonite-zoisite-aragonite as well as for aragonite coexisting with a fluid with a mole fraction of H_2O of 0.40. It should be noted that in this case identical $\mu(H_2O)$'s are calculated for two different phase assemblages. (3) Addition of CO_2 component to a H_2O-undersaturated – fluid-absent assemblage, might increase the chemical potential of H_2O, as shown by the arrow from point A to point B (Fig. 7a). At point A, grossular-zoisite-aragonite coexist, $\mu(H_2O)$ is −249 kJ. From point A to point B, the content of CO_2 in the bulk composition increases and at point B zoisite-lawsonite-aragonite coexist with a $\mu(H_2O)$ of −243 kJ. It should be noted that in this particular case an increase of CO_2 in the bulk composition causes an increase of the number of hydrous phases present.

Fig. 7a also shows that for low-temperature – high-pressure conditions lawsonite or zoisite coexist only with fluids rich in H_2O. At higher temperatures (Fig. 7b and c), zoisite may coexist with relatively CO_2 rich fluids. This latter result is in accordance with the occurrence of zoisite in metacarbonates.

In conclusion, we suggest that the result of "multi-equilibrium" calculations can be misleading if the stability of the assemblage is not completely tested. In such "multi-equilibrium" calculations, "calculated $X(H_2O)$" are based on the assumption that a fictitious fluid phase was present. However, such a fictitious fluid phase is not mandatory and calculated $\mu(H_2O)$ which result in water-undersaturation might equally be interpreted as H_2O-undersaturated – fluid-absent conditions. Further caution in the interpretation of calculated $X(H_2O)$ is suggested by the possible presence of inert components in the fluid, which may lead to dramatic effects on topology (Trommsdorff and Evans 1977).

The use of zoisite in geothermobarometry

Zoisite is an excellent and ubiquitous buffer for both grossular component in garnet and anorthite component in plagioclase over a wide range of metamorphic conditions according to reactions (1), (3), (5), and

$$15 \text{ diopside} + 12 \text{ zoisite} = 13 \text{ grossular} + 5 \text{ pyrope} + 12 \text{ quartz/coesite} + 6\ H_2O. \quad (11)$$

Equilibrium (5) was studied by Goldsmith (1982) with anorthite diluted in plagioclase solid solution. Its geothermometric application is mainly devoted to relatively low pressure conditions. Equilibria (3) and (10) were successfully used by Okay (1995), O'Brien (1993), Chopin et al. (1991), and Poli and Schmidt (1995, 1997) to depict phase relationships both in natural and synthetic garnet amphibolites and eclogites.

Figure 8 was calculated with Vertex, using the database of Berman (1988), EoS for water by Delany and Helgeson (1978) and the solution model of Berman (1990) for garnet. It should be noted that Fig. 8 differs from Fig. 6 in Okay (1995) by the fact that we do not use fixed activity calculations in the model system CASH but we derive the grossular component in garnet in

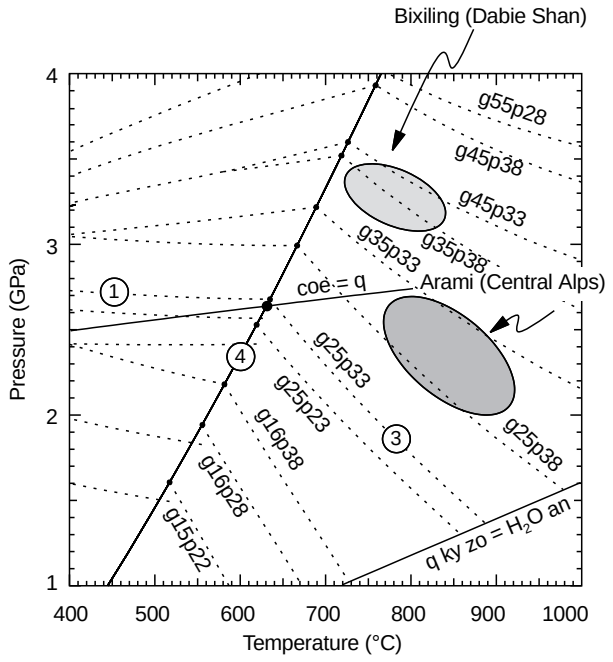

Fig. 8 Geobarometers zoisite = lawsonite + grossular + kyanite + quartz/coesite (reaction 1) and zoisite = grossular + kyanite + quartz/coesite + H_2O (reaction 3) calculated using thermodynamic properties for zoisite given in this study and the model of Berman (1990) for garnet. Reaction 4 is the breakdown of lawsonite as described in text, Fig. 3, and Fig. 5. *Isopleths* indicate garnet compositions represented by percentage of grossular (*g*) and pyrope (*p*) components in ternary Fe-Mg-Ca garnet solid solution, i.e. g25p33 = 25% grossular, 33% pyrope, 42% almandine. Metamorphic conditions for Dabie-Shan terrains are evaluated after data given in Okay (1995) and Zhang et al. (1995), and for Arami (Central Alps) after Heinrich (1986)

equilibrium with the other components in garnet in a CFMASH system (following the "pseudo-compounds" approximations, see Connolly 1990; Connolly and Kerrick 1987). Pyrope component in blueschists or orogenic eclogites usually varies from 15 mol% to 35 mol% (Carswell 1990); such pyrope contents in garnets are reproduced by our calculation in Fig. 8.

Both equilibria (3) and (11) have a moderate dP/dT slope. In *P-T* space, reaction (3) is slightly positive in the model system CASH (hydration with increasing *T*, see above) but becomes progressively negative (dehydration with increasing *T*) with increasing dilution of grossular component in garnet. As a result, at typical crustal conditions (Fig. 8) this reaction becomes rather steep in *P-T* space and its application for pressure estimates is not reliable unless temperature is well constrained. Reaction (11), where kyanite is replaced by pyrope minus diopside, has the advantage of a flatter slope in *P-T* space and a general applicability for eclogites equilibrated both in the quartz and in the coesite field. Unfortunately, a general and simple graphic representation as in Fig. 8 cannot be presented for reaction (11) because diopside activity is controlled by X_{Mg}-ratio and jadeite component in clinopyroxene which both vary significantly in natural rocks. Our retrieved thermodynamic data for zoisite can be used for computation of the location of this equilibrium at user defined diopside activities.

In the H_2O-undersaturated region, reaction (1) constitutes a useful geobarometer. However, zoisite being regarded in most petrographic analysis as a replacement product of lawsonite, a small number of case studies propose the coexistance of zoisite and lawsonite (e.g. Barnicoat 1988).

Concluding statements

1. The stability of zoisite is limited through a water-absent reaction at pressures between 5.0 GPa (at 700 °C) and 6.6 GPa (at 950 °C).
2. Employing measured crystallophysical properties (bulk moduli, thermal expansivities, and C_P-functions, the latter being dependant on bulk modulus and thermal expansivity at high temperatures), sets of thermodynamic properties for zoisite and lawsonite can be derived consistent with our high-pressure experiments and consistent with previous low-pressure – high-temperature experiments.
3. Zoisite occurs at H_2O-saturated conditions, at H_2O-undersaturated – fluid-absent and at H_2O-undersaturated – mixed-fluid (CO_2-H_2O) conditions. Thus, equilibria involving zoisite can be employed as geohygrometers. The calculation of multiple metamorphic equilibria on the basis of solid phase compositions yields a $\mu(H_2O)$. For H_2O-undersaturated conditions, the calculated $\mu(H_2O)$ is not necessarily a result of the presence of a mixed CO_2-H_2O fluid, it could equally result from the absence of a fluid phase.
4. The presence of zoisite in eclogite facies rocks provides a buffer for grossular content in garnet. Thus, the equilibrium zoisite + diopside = garnet + quartz/coesite + H_2O constitutes an excellent geobarometer for low- to medium-temperature eclogites.

Acknowledgements Most multi-anvil experiments were performed at the Bayerisches Geoinstitut under the EC Human Capital and Mobility – Access to Large Scale Facilities programme (contract ERBCHGECT940053 to D.C. Rubie). S.P.'s work was also supported by MURST-40% grants and CNR-95.04174.CT11/95.00412.CT05 fundings. The authors are grateful for constructive reviews by K.D. Grevel and J.G. Liou.

References

Akaogi M, Yusa H, Shiraishi K, Suzuki T (1995) Thermodynamic properties of a-quartz, coesite, and stishovite and equilibrium phase relations at high pressures and high temperatures. J Geophys Res 100: 22337–22347

Anderson DL (1989) Theory of the Earth. Blackwell, Oxford

Barnicoat AC (1988) Zoned high-pressure assemblages in pillow lavas of the Zermatt-Saas ophiolite zone, Switzerland. Lithos 21: 227–236

Berman RG (1988) Internally consistent thermodynamic data for minerals in the system Na_2O-K_2O-CaO-MgO-FeO-Fe_2O_3-Al_2O_3-SiO_2-TiO_2-H_2O-CO_2. J Petrol 29: 445–522

Berman RG (1990) Mixing properties of Ca-Mg-Fe-Mn garnets. Am Mineral 75: 328–344

Berman RG (1991) Thermobarometry using multi-equilibrium calculations: a new technique, with petrological applications. Can Mineral 29: 833–855

Berman RG, Brown TH (1985) Heat capacity of minerals in the system Na_2O-K_2O-CaO-MgO-FeO-Fe_2O_3-Al_2O_3-SiO_2-TiO_2-H_2O-CO_2: representation, estimation, and high temperature extrapolation. Contrib Mineral Petrol 89: 168–183

Boettcher AL (1970) The system CaO-Al_2O_3-SiO_2-H_2O at high pressures and temperatures. J Petrol 11: 337–379

Bohlen SR, Boettcher AL (1982) The quartz-coesite transformation: a precise determination and the effects of other components. J Geophys Res 87: 7073–7078

Brodholt JP, Wood BJ (1993) Simulation of the structure and thermodynamic properties of water at high pressure and temperature. J Geophys Res 98: 519–536

Carswell DA (1990) Eclogites and the eclogite facies: definitions and classifications. In: Carswell DA (ed) Eclogite facies rocks. Blackie, New York, pp 1–13

Chatterjee ND, Johannes W, Leistner H (1984) The system CaO-Al_2O_3-SiO_2-H_2O: new phase equilibria data, some calculated phase relations, and their petrological applications. Contrib Mineral Petrol 88: 1–13

Chopin C, Henry C, Michard A (1991) Geology and petrology of the coesite-bearing terrain, Dora Maira massif, Western Alps. Eur J Mineral 3: 263–291

Comodi P, Zanazzi PF (1996) Effects of temperature and pressure on the structure of lawsonite. Am Mineral 81: 833–841

Comodi P, Zanazzi PF (1997) The pressure behaviour of clinozoisite and zoisite: an X-ray diffraction study. Am Mineral 82: 61–68

Comodi P, Zanazzi PF, Poli S, Schmidt MW (1997) High pressure behaviour of kyanite: compressibility and structural deformations. Am Mineral 82: 452–459

Connolly JAD (1990) Multivariable phase diagrams: an algorithm based on generalized thermodynamics. Am J Sci 290: 666–718

Connolly JAD, Kerrick DM (1987) An algorithm and computer program for calculating composition phase diagrams. CALPHAD 11: 1–55

Davies JH, Stevenson DJ (1992) Physical model of source region of subduction zone volcanics. J Geophys Res 97: 2037–2070

Deer WA, Howie RA, Zussman J (1986) Epidote group. In: Deer WA, Howie RA, Zussman J. Disilicates and ring silicates, Longman, Harlow, pp 2–179

Delany JM, Helgeson HC (1978) Calculation of the thermodynamic consequences of dehydration in subducting oceanic crust to 100 kbar and >800 °C. Am J Sci 278: 638–686

Domanik KJ, Holloway JR (1997) The stability and composition of phengitic muscovite and associated phases from 5.5–11 GPa: implications for deeply subducted sediments. Geochim Cosmochim Acta 60: 4133–4150

Fei Y (1995) Thermal expansion. In: Ahrens TJ (ed) Mineral physics and crystallography. Am Geophys Union Ref Shelf 2, Washington, DC pp 29–44

Frost DJ, Wood BJ (1997) Experimental measurements of the properties of H_2O-CO_2 mixtures at high pressures and temperatures. Geochim Cosmochim Acta (in press)

Ghent ED (1988) Tremolite and H_2O activity attending metamorphism of hornblende-plagioclase-garnet assemblages. Contrib Mineral Petrol 98: 163–168

Goldsmith JR (1982) Plagioclase stability at elevated temperatures and water pressures. Am Mineral 67: 653–675

Gordon TM (1973) Determination of internally consistent thermodynamic data from phase equilibrium experiments. J Geol 81: 199–208

Grevel KD, Burchard M, Fasshauer D (1996) In situ diffraction investigations of diaspore, lawsonite, and pyrophillite with MAX-80 using synchrotron radiation (abstract). Terra Nova 8 Abstr Suppl 1: 24

Halbach H, Chatterjee ND (1982) An empirical Redlich-Kwong-type equation of state for water to 1000 °C and 200 kbar. Contrib Mineral Petrol 79: 337–345

Heinrich CA (1986) Eclogite facies regional metamorphism of hydrous mafic rocks in the central alpine Adula nappe. J Petrol 27: 123–154

Helgeson HC, Delaney JM, Nesbitt HW, Bird DK (1978) Summary and critique of the thermodynamic properties of rock-forming minerals. Am J Sci 278A: 1–229

Holland TJB, Powell R (1990) An enlarged and updated internally consistent thermodynamic dataset with uncertainties and correlations: the system K_2O-Na_2O-CaO-MgO-MnO-FeO-Fe_2O_3-Al_2O_3-TiO_2-SiO_2-C-H_2-O_2. J Metamorphic Geol 8: 89–124

Holland TJB, Powell R (1991) A compensated-Redlich-Kwong (CORK) equation for volumes and fugacities of CO_2 and H_2O in the range 1 bar to 50 kbar and 100–1600 °C. Contrib Mineral Petrol 109: 265–273

Holland TJB, Redfern SAT, Pawley AR (1996) Volume behaviour of hydrous minerals at high pressure and temperature. II. Compressibilities of lawsonite, zoisite, clinozoisite, and epidote. Am Mineral 81: 341–348

Jenkins DM, Newton RC, Goldsmith JR (1985) Relative stability of Fe-free zoisite and clinozoisite. J Geol 93: 663–672

Katsura T, Ito E (1989) The system Mg_2SiO_4-Fe_2SiO_4 at high pressures and temperatures: precise determination of the stabilities of olivine, modified spinel and spinel. J Geophys Res 94: 15663–15670

Knittle E (1995) Static compression measurements of equations of state. In: Ahrens TJ (ed) Mineral physics and crystallography. Am Geophys Union Ref Shelf 2, Washington, DC, pp 98–142

Levien L, Prewitt CT (1981) High pressure crystal structure and compressibility of coesite. Am Mineral 66: 324–333

Li B, Ridgen SM, Liebermann RC (1997) Elasticity of stishovite at high pressure. Phys Earth Planet Inter (in press)

Libowitzky E, Armbruster T (1995) Low-temperature phase transitions and the role of hydrogen bonds in lawsonite. Am Mineral 80: 1277–1285

Newton RC (1966) Some calc-silicate equilibrium relations. Am J Sci 264: 204–222

Manning CE (1994) The solubility of quartz in H_2O in the lower crust and upper mantle. Geochim Cosmochim Acta 58: 4831–4839

Nicholls IA, Ringwood AE (1973) Effect of water on olivine stability in tholeiites and the production of silica-saturated magmas in the island-arc environment. J Geol 81: 285–300

O'Brien PJ (1993) Partially retrograded eclogites of the Münchberg Massif, Germany: records of a multistage Variscan uplift history in the Bohemian Massif. J Metamorphic Geol 11: 241–260

Okay AI (1995) Paragonite eclogites from Dabie Shan, China: re-equilibration during exhumation? J Metamorphic Geol 13: 449–460

Pawley AR (1994) The pressure and temperature stability limits of lawsonite: implications for H_2O recycling in subduction zones. Contrib Mineral Petrol 118: 99–108

Pawley AR, Redfern SAT, Holland TJB (1996) Volume behaviour of hydrous minerals at high pressure and temperature. I. Thermal expansion of lawsonite, zoisite, clinozoisite, and diaspore. Am Mineral 81: 335–340

Perkins D III, Westrum EF Jr, Essene EJ (1980) The thermodynamic properties and phase relations of some minerals in the system CaO-Al_2O_3-SiO_2-H_2O. Geochim Cosmochim Acta 44: 61–84

Pistorius CW, Kennedy GC, Sourirajan S (1962) Some relations between the phases anorthite, zoisite, and lawsonite at high temperatures and pressures. Am J Sci 260: 44–56

Poli S, Schmidt MW (1995) H_2O transport and release in subduction zones: experimental constraints on basaltic and andesitic systems. J Geophys Res 100: 22299–22314

Poli S, Schmidt MW (1997) The high pressure stability of hydrous phases in orogenic belts: an experimental approach on eclogite forming processes. Tectonophysics 273: 169–184

Powell R, Holland T (1994) Optimal geothermometry and geobarometry. Am Mineral 79: 120–133

Rice JM, Ferry JM (1982) Buffering, infiltration, and the control of intensive variables during metamorphism. In: Ferry JM (ed) Characterization of metamorphism through mineral equilibria. (Reviews in mineralogy, vol 10) Mineral Soc Am, Washington, DC, pp 263–326

Robie RA, Hemingway BS, Fisher JR (1978) Thermodynamic properties of minerals and related substances at 298.15 K and 1 bar (10^5 pascals) pressure and at higher temperatures. US Geol Surv Bull 1452

Rubie DC (1990) Role of kinetics in the formation and preservation of eclogites. In: Carswell DA (ed) Eclogite facies rocks. Blackie, New York, pp 111–140

Saxena SK, Fei Y (1987a) Fluids at crustal pressure and temperatures. I. Pure species. Contrib Mineral Petrol 95: 370–375

Saxena SK, Fei Y (1987b) High pressure and high temperature fluid fugacities. Geochim Cosmochim Acta 51: 783–792

Saxena SK, Chatterjee N, Fei Y, Shen G (1994) Thermodynamic data on oxides and silicates. Springer-Verlag, Berlin Heidelberg New York

Schmidt MW (1995) Lawsonite: upper stability and formation of higher density hydrous phases. Am Mineral 80: 1286–1292

Schmidt MW, Poli S (1994) The stability of lawsonite and zoisite at high pressures: experiments in CASH to 92 kbar and implications for the presence of hydrous phases in subducted lithosphere. Earth Planet Sci Lett 124: 105–118

Schmidt MW, Poli S, Comodi P, Zanazzi PF (1997) High pressure behaviour of kyanite: decomposition of kyanite into stishovite and corundum. Am Mineral 82: 460–466

Skrok V, Grevel KD, Schreyer W (1994) Die Stabilität von Lawsonit, $CaAl_2[Si_2O_7](OH)_2{\cdot}H_2O$, bei Drücken bis zu 50 kbar. Eur J Mineral 6: 270

Smith DC (1988) A review of the peculiar mineralogy of the "Norwegian coesite-eclogite Province", with crystal-chemical, petrological, geochemical and geodynamical notes and an extensive bibliography. In: Smith DC (ed) Eclogites and eclogite-facies rocks. (Developments in petrology, vol 12) Elsevier, Amsterdam, pp 1–206

Susaki J, Akaogi M, Akimoto S, Shimura O (1985) Garnet-perovskite transformation in $CaGeO_3$: in-situ X-ray measurements using synchrotron radiation. Geophys Res Lett 12: 729–732

Thompson AB, Ellis DJ (1994) $CaO + MgO + Al_2O_3 + SiO_2 + H_2O$ to 35 kbar: amphibole, talc, and zoisite dehydration and melting reactions in the silica-excess part of the system and their possible significance in subduction zones, amphibolite melting, and magma fractionation. Am J Sci 294: 1229–1289

Thompson AB, Perkins D (1981) Lambda transitions in minerals. In: Newton RC, Navrotsky A, Wood BJ (eds) Thermodynamics of minerals and melts. (Advances in Physical Geochemistry, vol 1) Springer, Berlin Heidelberg New York, 35–62

Trommsdorff V, Evans BW (1977) Antigorite-ophicarbonates: phase relations in a portion of the system CaO-MgO-SiO_2-H_2O-CO_2. Contrib Mineral Petrol 60: 39–56

Winter JK, Ghose S (1979) Thermal expansion and high-temperature crystal chemistry of the Al_2SiO_5 polymorphs. Am Mineral 64: 573–586

Wunder B, Rubie DC, Ross NL, Medenbach O, Seifert F, Schreyer W (1993) Synthesis, stability, and properties of $Al_2SiO_4(OH)_2$: a fully hydrated analogue of topaz. Am Mineral 78: 285–297

Yagi T, Akaogi M, Shimomura O, Suzuki T, Akimoto SI (1987) In-situ observation of the olivine-spinel phase transformation in Fe_2SiO_4 using synchrotron radiation. J Geophys Res 92: 6207–6213

Zhang J, Li B, Utsumi W, Liebermann RC (1996) In situ X-ray observations of the coesite-stishovite transition: reversed phase boundary and kinetics. Phys Chem Miner 23: 1–10

Zhang RY, Liou JG, Cong BL (1995) Talc-, magnesite- and Ti-clinohumite-bearing ultrahigh-pressure metamafic and ultramafic complex in the Dabie Mountains, China. J Petrol 36: 1011–1037